System Optimization to Eliminate Chirping in Dual Drive $LiNbO_3$ MZM at 40 Gb/s

Nazmi A. Mohammed[*], Yasmine El-Guindy[**] , Moustafa H. Aly(OSA Member)[***]

[*]Research Centre, Smart Village, College of Engineering and Technology, Arab Academy For Science, Technology and Maritime Transport, Cairo, Egypt

[**]Department of Electronics and Communications Engineering, College of Engineering and Technology, Arab Academy For Science, Technology and Maritime Transport, Cairo, Egypt

ABSTRACT:

The chirping performance of dual drive lithium Niobate (LiNbO3) Mach–Zehnder modulators (MZM) at 40 Gb/s non-return to zero (NRZ) data signal is investigated along with the effect of various filtering techniques. The chirping performance is evaluated then enhanced by optimizing the design parameters (bias voltage and the extinction ratio). Also while comparing the results of the unfiltered and filtered signals; it shows that the chirp parameter can decrease from 0.41 to 0.15 at the push-pull operation. Also a remarkable 100 Hz chirping amplitude is achieved with Bessel filtering, half wave voltage ($V\pi$ = 4 V), push pull operation and an extinction ratio of 20 dB.

Keywords **-** Mach-Zehnder Modulator; Lithium Niobate; Chirp; Extinction Ratio; Bias Voltage; Filters.

I. INTRODUCTION

As the demand for telecommunication services, bandwidth and high bit rates have boomed, modulators have started playing an important role in the telecommunication process due to their importance in high bit rate lightwave systems [1]. The most widely used modulator in optical transmitters is the Mach-Zehnder modulator (MZM) which is based on the Mach-Zehnder interferometer (MZI). The advantages of the MZM are eliminating pulse, spectral broadening and having a controllable chirp [2]. The disadvantages of the MZM like all other external modulators are their design complexity and optical loss [3]. The advantages of the $LiNbO_3$ MZM over other electro-optic modulators are the low losses, large extinction ratio, low chirp and small wavelength dependence which make them suitable for dense wavelength multiplexing (DWDM) [4-6]. Chirping is considered the most important parameter that affects the MZM which causes undesired frequency variation due to its interaction with dispersive effects that distort the data signal [7]. Sometimes, it is preferred to have an adjustable chirp in order to decrease the transmission penalties in optical communication systems [5and 8].

The chirping performance of a 10 Gb/s NRZ system based on single and dual arm $LiNbO_3$ MZM has been investigated by John C. Cartledge et al. [8]. The study has been done by varying the splitting ratio between the arms of the modulator and its influence on the extinction ratio and consequently their effect on the chirping phenomena. Paolo Bravetti et al. [9] studied the theoretical and experimental chirp values of a dual drive $LiNbO_3$ MZM operating at 10 Gb/s for a NRZ system.

Unbalancing the optical power in the two arms of the MZM proved that the chirp induced does not produce any spectral broadening of the transmitted spectrum. The relation between the driving voltage ratio and the chirping factor has been studied. The performance and cost effectiveness of a single arm 10 Gb/s MZM in a 42.7 Gb/s transmitter has been investigated by Douglas M. Gill, et al. [10]. The used MZM is a commercial one and has shown that the MZM-low pass filter (LPF) duobinary approach in conjunction with optical filtering may provide significant cost savings for a high spectral efficiency transmission since the 10 Gb/s MZM can be used for 40 Gb/s transmission.

The present work explores to the author's best knowledge for the first time, the effect of filtering NRZ input data signals on the chirping performance of a dual drive MZM at 40 Gb/s operation. This study includes the effect of the extinction ratio and biasing voltage, combined, on the modulator chirping performance at 40 Gb/s.

This work is organized as follows: Section 2 presents the basic operation and mathematical model. Results that explore the effect of the previously mentioned parameters on chirping phenomena will be discussed in Sec. 3, followed by the conclusion in Sec. 4.

II. BASIC OPERATION AND MATHEMATICAL MODEL

2.1 Basic Operation

The structure of an MZM consists of an input waveguide followed by a Y-junction that splits the optical signal between the upper and lower arms and combiner to recombine the modulated signals of the two arms. Figure 1 shows the operation of intensity MZM. In MZMs, the incoming light splits into two waveguides under the influence of conducting electrodes, as shown in Fig.1. The electro-optical effect induces a change in the refractive index of each interferometer arm and the phase modulates the light that is propagating into that arm according to the electric voltage applied to each electrode. By combining the two paths with different phase modulations, this phase modulation is turned into an intensity modulation [11].

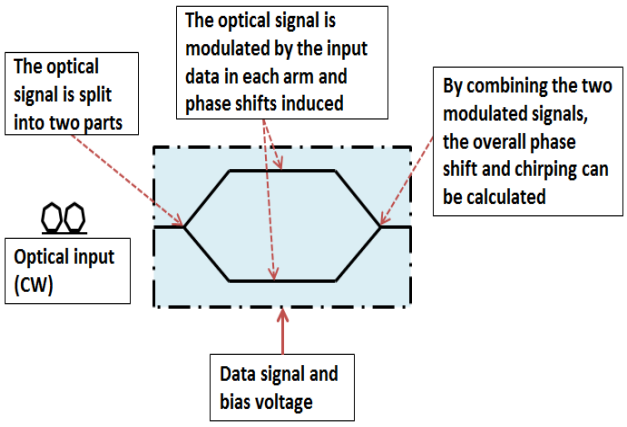

Fig. 1 MZM operation.

2.2 Mathematical Model

In the most general case, it is assumed that the phase shift experienced by the two arms depends on the voltages applied to the upper and lower arms and that they can be created independently [12]. The field at the output of the modulator is the sum of the contributions propagating through the upper and lower paths. Therefore, its complex envelope can be expressed as

$$E_{out}(t)=e^{-j\phi'}(ae^{-j\frac{\Delta\phi}{2}}+be^{j\frac{\Delta\phi}{2}})E_{in}(t) \quad (1)$$

$$a=\rho_1\sqrt{\alpha}\sqrt{\beta} \quad (2)$$

$$b=\rho_2\sqrt{1-\alpha}\sqrt{1-\beta} \quad (3)$$

$$\Delta\phi=\phi_1-\phi_2 \quad (4)$$

$$\phi'=\frac{\phi_1-\phi_2}{2} \quad (5)$$

where ϕ_1 , ϕ_2 are the phase shifts of the upper/lower arm of the modulator, α, β are the power splitting ratios of the input/output Y-junction and ρ_1, ρ_2 are the insertion losses at the input/output Y-junction, respectively.

So, the general expression for the field at the output of the modulator by expanding (1) using Euler's formula is

$$E_{out}(t)=E_{in}(t)e^{-j(\phi'+\Psi)}\sqrt{(a+b)^2\cos^2\frac{\Delta\phi}{2}+j(a-b)^2\sin^2\frac{\Delta\phi}{2}} \quad (6)$$

where X is the phase term, which depends on the power imbalance between the upper and lower arms of the interferometer.

The voltage applied to each arm of the interferometer can be written as the sum of a dc and an ac term

$$V_1(t)=V_{dc_1}+V_{pp_1}d_1(t) \quad (7)$$

$$V_2(t)=V_{dc_2}+V_{pp_2}d_2(t) \quad (8)$$

where $V_{pp}(i)$ is the peak-to-peak voltage of the signal applied to the arm i, and di (t) is its normalized waveform such that di(t) ∈ [-0.5, 0.5].

$$E_{out}(t)=\sqrt{P_{out}(t)}e^{-j\phi(t)} \quad (9)$$

$$P_{out}(t)=P_{in}(t)\rho^2\cos^2[\frac{\pi}{2V_\pi}\{V_{dc1}-V_{dc2}+V_{pp1}d_1(t)-V_{pp2}d_2(t)\}] \quad (10)$$

and

$$\phi(t) = [\frac{\pi}{2V_\pi}\{V_{dc1} + V_{dc2} + V_{pp1}d_1(t) + V_{pp2}d_2(t)\}] \quad (11)$$

The extinction ratio (ER) is the ratio between the output optical power corresponding to the maximum transmission value and the minimum transmission value. It can be calculated as follows:

$$ER = \frac{P_{\max}}{P_{\min}} \quad (12)$$

while assuming that, the splitting ratio and combining ratio = 0.5 and after simplification, one can write the extinction ratio in terms of the insertion loss (ρ) as

$$ER = 10^{\frac{\rho}{20}} \quad (13)$$

The chirping parameter, α, of an MZM is defined by [12]

$$\alpha = -[\frac{\frac{d\phi}{dt}}{\frac{1}{2P}\frac{dP}{dt}}] \quad (14)$$

$$\alpha = \cot[\frac{\pi}{2V_\pi}\{\Delta V_{bias} + 2V_{pp}d(t)\}] \quad (15)$$

Where V_{bias} is the biasing voltage and it depends on the difference between the two input dc voltages.

By Simplifying Eq. (15) and assuming the modulator arms are symmetric, the parameter α is obtained as [14]

$$\alpha = \frac{V_2 + V_1}{V_2 - V_1} \quad (16)$$

III. RESULTS AND DISCUSSION

3.1 Introduction

In $LiNbO_3$ modulators, the Kerr effect is negligible and the Pockels effect is dominant. The chirping in $LiNbO_3$ Mach-Zehnder modulators is mainly due to the imbalance between the modulation depths in the two arms of the Mach-Zehnder waveguides. The higher order modulation sideband components are not due to the Kerr effect; they are due to successive optical phase modulation through the Pockels effect. The chirping effect is proportional to the transmitted signal power as it affects the high power systems severely. A well-controlled frequency chirp can be beneficial for transmission [12].

Figure 2 shows the optical transmitter used to test and investigate the effect of filtering windows, extinction ratio and bias voltage on the chirping performance of a dual drive $LiNbO_3$ MZM at 40 Gb/s NRZ operation. The transmitter consists of a bit sequence generator as a data source, a continuous wave (CW) laser as a laser source, an NRZ pulse generator, filters and an MZM. Specifications of the data source, NRZ pulse generator and the laser source are listed in Table. 1 as referenced in [2].

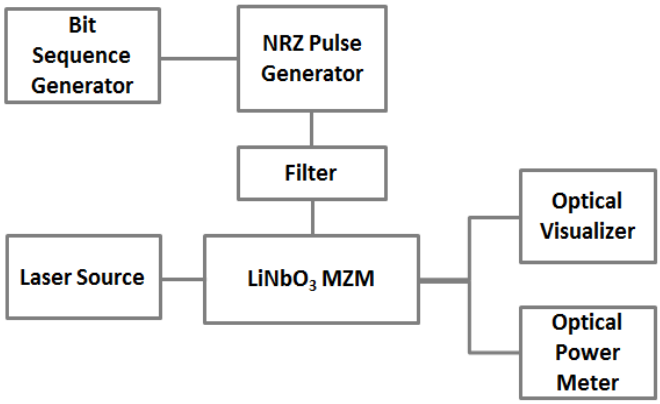

Fig. 2 Schematic diagram of the transmitter.

Table 1 Values of transmitter components.

Device	Specifications
Bit sequence generator	16 bit
NRZ pulse generator	Rectangular Rise time: 0.1 bit Fall time: 0.1 bit
CW laser	Power: 0 dBm Center Emission Frequency: 193.1THz Wavelength: 1550 μm

3.2 Filtering effect

Dispersion, attenuation and nonlinearities are considered the main impairments that degrade the performance of optical networks [13]. As mentioned before the chirping phenomenon is considered one of the problems that arise in optical modulators. It is preferred that frequency chirping be avoided in optical transmitters for long distance transmission since it broadens the spectrum and limits the spectral efficiency [13]. Furthermore, MZMs require chirp-free operation, strict conditions are therefore imposed on the voltage imbalance and delay between the signals driving each of the arms of the modulator [12]. In digital communication filtering the input data enhances the characteristics of the transmitted data through the digital link [14]. In this section the effect of filtering digital input data signal on the chirping performance of the dual drive $LiNbO_3$ MZM will be tested at 40 Gb/s operation with switching voltage (V_π = 4 V) and (ER= 15 dB). The previous values for V_π and ER were chosen based on initial values from other literatures [2 and 15] and ER is later optimized in a section that follows. Ripples introduced from filtering on the modulated signal are also addressed.

Figure 3.a represents the NRZ signal generated after the combination of the input digital bit sequence and the NRZ pulse as shown in Fig 2. Figure 3.b (with double Y-axes) is the output displayed in the optical time domain visualizer and it shows an NRZ bit stream modulated by a CW laser source and a $LiNbO_3$ MZM. The output signal is accompanied by chirping signal amplitude of about 10 GHz which is quite large for the 40 Gb/s modulation and can effectively degrade the transmitter performance, especially in long distance transmission.

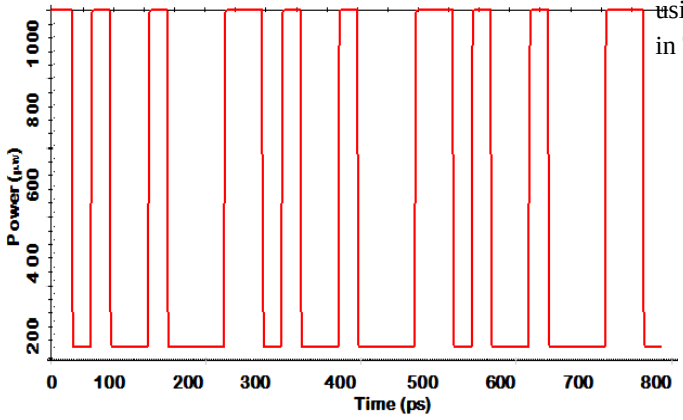

(a)

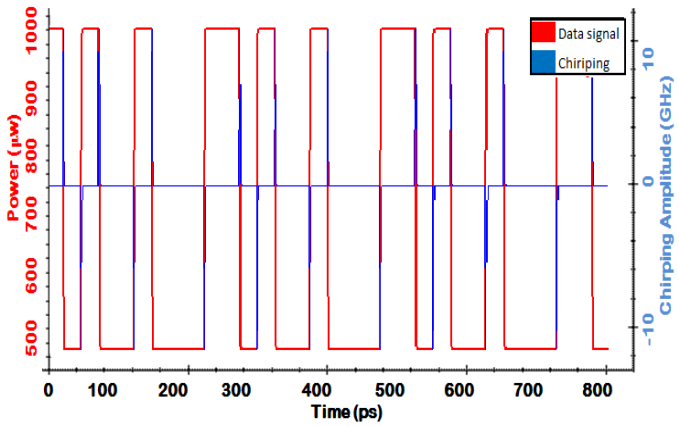

(b)

Fig.3 a) Input NRZ digital data signal. b) MZM output optical data with no filtering.

By applying different filtering techniques to the digital input data, an enhancement in the chirping performance for the $LiNbO_3$ MZM at 40 Gb/s modulation is observed. Figure 4(a-d) shows the modulated NRZ bit stream and chirping spectrum after applying different filtering techniques. It is thought that the enhancement in the chirping performance is due to the improvement in the phase shift of the output modulated signal resulting from filtering. This shows fair agreement with the mathematical background as shown in Eqs. (9) and (14). It is observed that filtering does not greatly affect the output power level of the modulated optical signal. The power lost, compared to the modulating signal power of 1 mW, is due to the imperfections in the material of the MZM's waveguide [12]. Values of chirping amplitude along with filter design parameters are tabulated in Table 2. The percentage of the modulated signal power to the modulating signal power is calculated using the optical power meter and values are listed in Table 2.

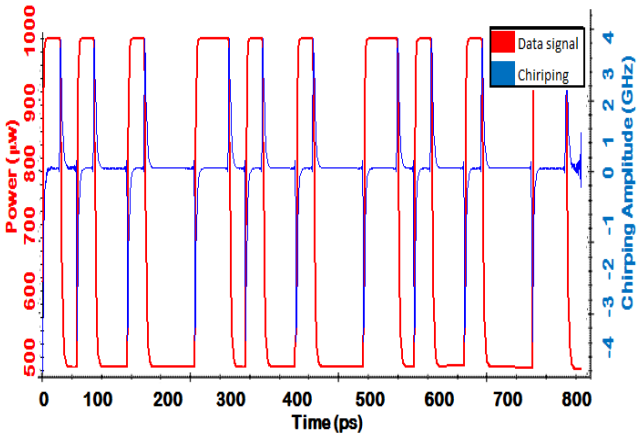

(a)

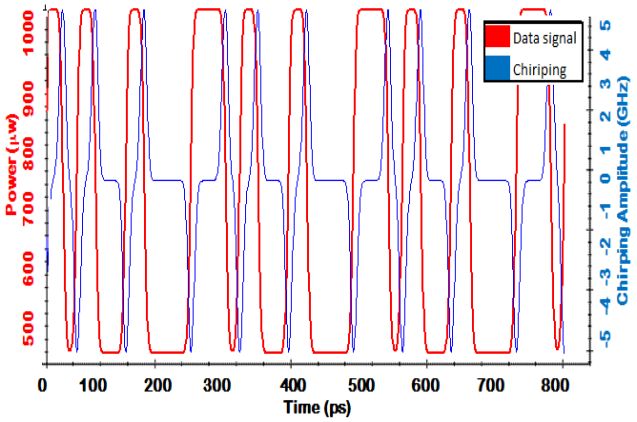

(b)

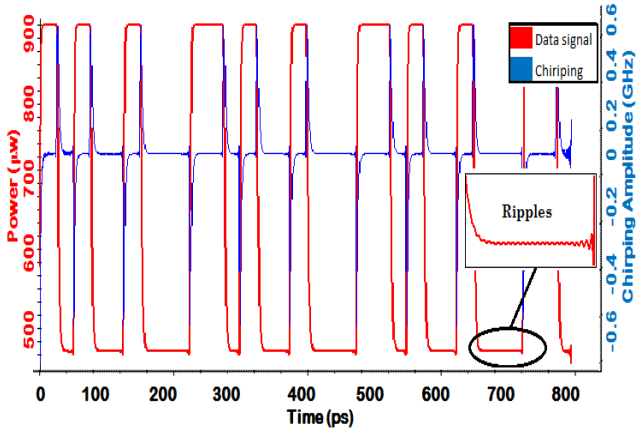

(c)

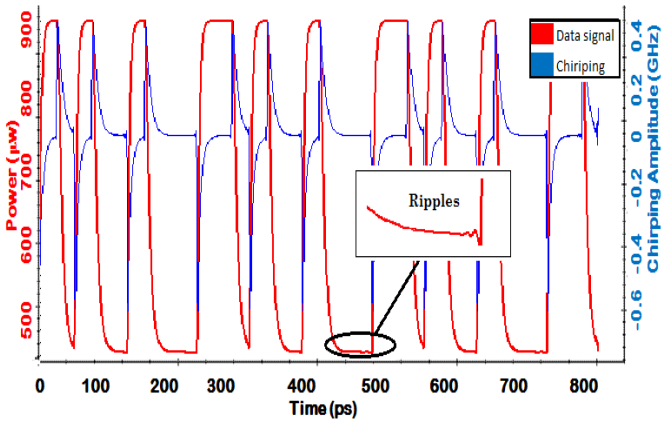

(d)

Fig. 4 MZM output showing the chirping amplitude with respect to the output data signal (a) Butterworth filter. (b) Gaussian filter. (c) Chebyshev filter. (d) Bessel filter.

According to Table 2 and Fig. 4, the Bessel filter shows an attractive chirping performance for the tested dual drive $LiNbO_3$ MZM at 40 Gb/s. Note that the observed chirping value (0.4 GHz) is quite high compared to previous literatures as mentioned in Table 3 section 3.4. The optimum chirping performance is observed with the Bessel filter followed by the Chebyshev, the Butterworth and the Gaussian filters, respectively. Minor effects of filtering windows on the measured output signal power were determined as shown in Table 2. In the following sections, discussion will be limited to Bessel filters since their attractive chirping performance arises through this section. Also, optimization of the ER and bias voltage will lead to remarkable chirping performance, especially with Bessel filtering.

Figure 5 shows the modulated optical signals using different filters at 40 Gb/s operation without chirping analysis. The spectrum provides a second view of the power of the modulated signal (accurate measurements are present above in Table 2). The figure also illustrates the ripples in the signal and a concurrence of bit durations between the no-filtering conditions and various filtering techniques. The Chebyshev and Bessel filters exhibit observable amplitudes of ripples as shown in figures 4 and 5, especially in the low level signal region; the Gaussian output signal, on the other hand, shows the greatest concurrency

with the no-filtering signal as well as a much lower chirping value as mentioned in Table 2.

Table 2 Experimental results of chirping performance and output power.

Filtering window	Filter specifications	Output power to input power (%)	Chirping amplitude (GHz)
Butterworth filter	Order = 1 Cut off frequency = 30 GHz Insertion loss = 0 dB	71.8	4
Gaussian filter	Order = 1 Cut off frequency = 30 GHz Insertion loss = 0 dB	71.6	5
Chebyshev filter	Order = 1 Cut off frequency = 30 GHz Insertion loss = 0 dB Ripple factor = 0.5 dB	69	0.6
Bessel filter	Order = 4 Cut off frequency = 30 GHz Insertion loss = 0 dB	71.4	0.4

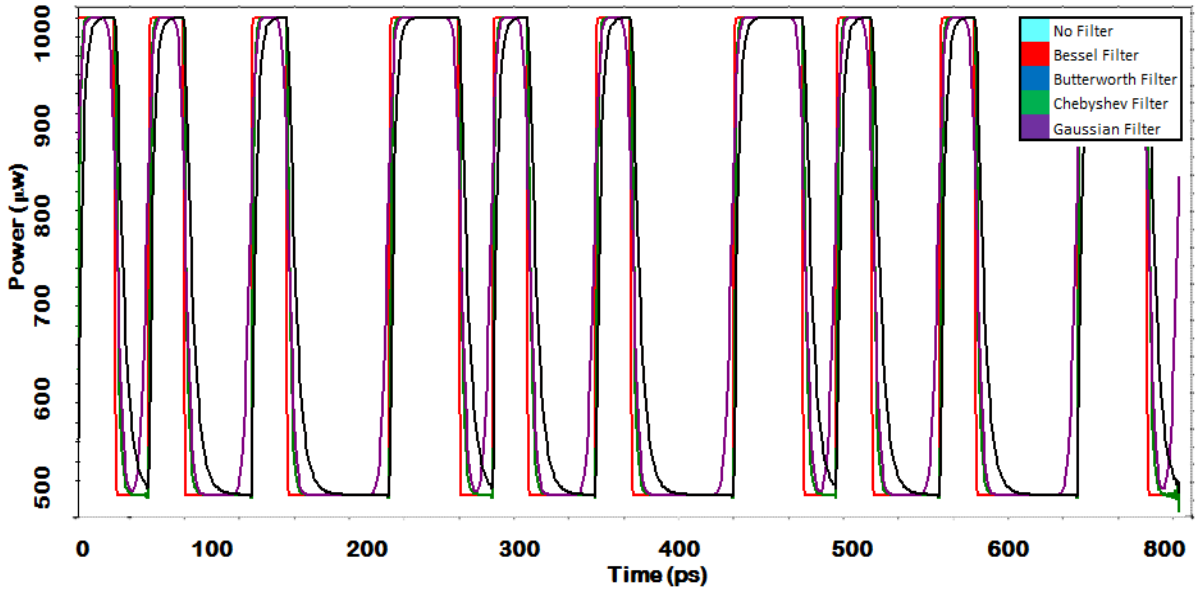

Fig.5 Comparison between different filtering windows.

3.3 Biasing Voltage Effect

The relation between the bias voltage and both the power and phase is represented in Eqs. (10), (11). The operation point is tuned with the bias voltage under normal operation to the quadrature point (push-pull operation). When the condition of push-pull operation is satisfied [$V_{bias1} = - V_{bias2} = V_{\pi}/2$] the phase shifts are, in theory, equal in magnitude but opposite in sign in the arms. A chirp-free intensity modulation is therefore obtained in which the chirping almost reaches zero [7 and 16]. To estimate the chirping performance of the tested modulator while applying different bias voltages, a Bessel filter which draws great attention due to its good chirping performance, (shown in the previous section) is used.

Figure 6 shows the relation between the biasing voltages applied to the two arms of the dual drive $LiNbO_3$ MZM at 40 Gb/s versus the α-parameter. As mentioned before, a free chirping operation should be observed if the condition of push-pull operation is satisfied. Experimental results show a fair agreement with the mathematical background explored in Section 2.2 by achieving a minimum value for the parameter α of 0.15 while using Bessel filter and 0.41 without any filter when the condition of push-pull

operation is satisfied for the tested dual drive $LiNbO_3$ MZM. Also, the results are consistent with the data tabulated in table 3 regarding the different speeds of similar modulators.

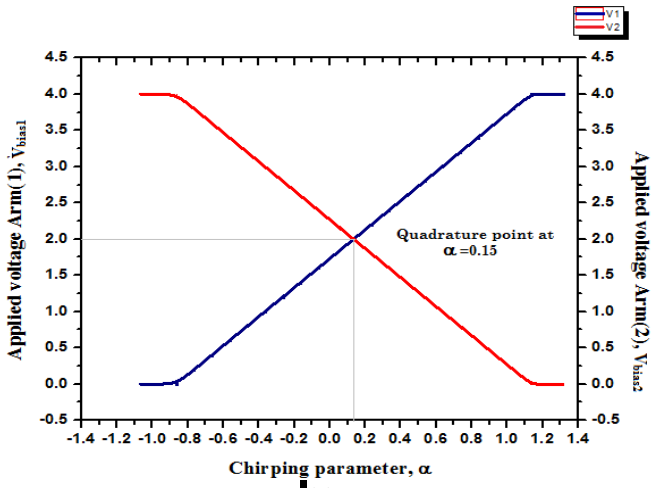

(a)

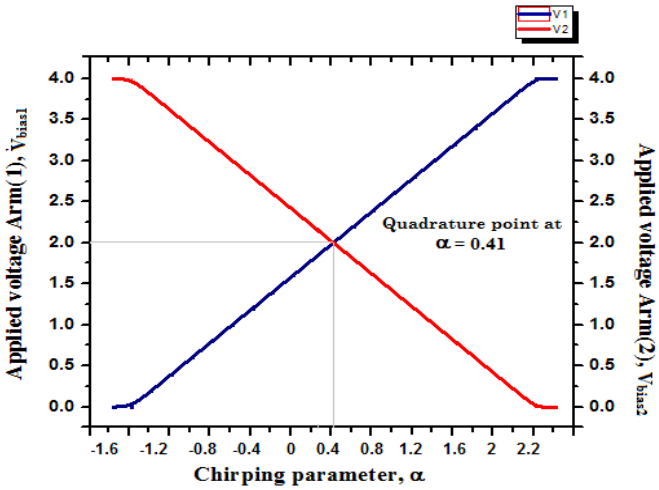

(b)

Fig.6 The relation between the input bias voltage and the parameter-α. (a) While using Bessel filter (b) without filtering.

3.4 Extinction Ratio Effect

To improve the performance of the MZM, a high separation between the high and low optical signal power levels is required [12]. The larger the modulation power, the easier it will be for the system receiver to accurately determine the corresponding signal level. As the extinction ratio should be maximized, one can assume an equal power split between the two arms of the interferometer and therefore, an infinite extinction ratio is obtained between the maximum and minimum power at the MZM. In practice, it is very difficult to obtain an equal power split between the MZM arms. So, in this section, we will investigate the impact of maximizing the extinction ratio with respect to the chirping amplitude.

An extinction ratio of 10 to 20 dB is a suitable design range according to similar modulators with different speeds tabulated in Table 3. To estimate the chirping performance of the tested modulator while varying the extinction ratio, a Bessel filter is used; also the modulator is operating under the push-pull operation condition.

Figure 7 shows the relation between the extinction ratio and the chirping amplitude for a dual drive $LiNbO_3$ MZM. From curve and based on the mentioned extinction ratio values, one can observe that, at extinction ratios 10 dB, 15 dB and 20 dB, the chirping amplitude reaches 4 GHz, 8 GHz and 100 Hz, respectively. So, the value of 20 dB will give a great optimization between the overall chirp amplitude and the high extinction ratio required to accurately distinguish between 0's and 1's at the receiver.

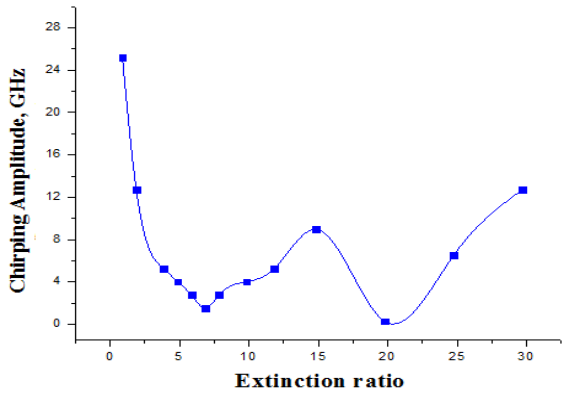

Fig. 7 Relation between the chirping amplitude and the extinction ratio.

Table 3 highlights the chirping performance for various types of $LiNbO_3$ MZMs under NRZ data format and different levels of bit rates. It also present the optimum design parameters (extinction ratio and bias point) required to achieve theoretical chirp-free performance. By exploring Table 3, an acceptable range of the α-parameter is from -0.2 to 0.75 for low bit-rate operations. However, according to our experiment which is carried out at 40 Gb/s, a better performance of 0.15 (which is lower than the performance of some of the modulators tabulated) can be achieved.

Table 3 Literature review on chirping performance for different MZMs.

Type of MZM	Material of MZM	Data format	Bit rate	Extinction ratio (dB)	Bias voltage (volt)	Chirp parameter for chirp free operation
Dual drive[15]	$LiNbO_3$	square/ sinusoidal /data bits	5GHz/ 5GHz /10Gb/s	14-30	V_{bias}=1.7-3 V_{π}=2.35	0.15-0.75
Dual drive [17]	NA	NRZ	10Gb/s	20	3/3.6 dB [1]	- 0.2
Dual drive[18]	$LiNbO_3$	NA	10Gb/s	23	V_{bias}=1.2/3.6 Vπ=2.35	0.15/0.19

[1] This value represents the difference between the maximum and minimum powers.

IV. CONCLUSION

This work presents a study of the effect of filtering techniques, bias voltage and the extinction ratio on the chirping performance of the dual drive $LiNbO_3$ MZM at 40 Gb/s. Bessel filters under the optimized design parameters (extinction ratio and bias point) achieve a remarkable 100 Hz chirping amplitude. The α-parameter is critical to optical communication systems because its interaction with chromatic dispersion introduces a limitation to the link distance without regenerating the signal; this work produced a remarkable α-parameter of 0.15 with 20 dB at a high bit-rate of 40 Gb/s, giving the optimized MZM high potential for long distance transmission.

REFERENCES

[1] G. P. Agrawal, Fiber Optic Communication Systems, 4th ed., New York (2010).

[2] Anu Sheetal, AjayK.Sharma and R.S.Kaler, "Impact of extinction ratio of single arm $\sin^2$ $LiNbO_3$ Mach–Zehnder modulator on the performance of 10 and 20 Gb/s NRZ optical communication system," Optik J. Light Elec. Optics, vol. 120, 2009, pp.704–709 (2009).

[3] H. Al-Raweshidy, Radio Over Fiber Technologies for Mobile Communications Networks, 1st ed., UK, 2002.

[4] Nadege courjal, Henri Porte, J.Hauden, P.Mollier and N.Grossard, "Modelling and optimization of low chirp LiNbo3 Mach-Zehnder modulators with an inverted ferroelectric domain section," J. Lightwave Technol., vol. 22, 2004, pp.1338-1343.

[5] C. E. Rogers III, J. L. Carini, J. A. Pechkis and P. L. Gould, "Characterization and compensation of the residual chirp in a Mach-Zehnder-type electro-optical intensity modulator," Opt. Express, vol. 18, 2010, pp. 1166-1176.

[6] Yuxin Wei, Yong Zhao, Jianyi Yang, Minghua Wang and Xiaoqing Jiang, "Chirp characteristics of silicon Mach–Zehnder modulator under small-signal modulation," J. Lightwave Technol., vol. 29, 2011, pp. 1011-1017 (2011).

[7] Giuseppe Pecere and Andrea Carena, "Spectral amplitude and phase characterization of optical devices," M.Sc. Thesis in Telecommunication Engineering by RF scan Telecommunication Engineering, Third School of Engineering: Information Technology of Politecnico di Torino, Italy, 2011.

[8] Antao Chen and Edmond J. Murphy, Broadband Optical Modulators: Science, Technology and Applications, 1st ed., New York, 2011.

[9] Paolo Bravetti, Stefano Balsamo, Jorge Alberto Villa Montoya, Raphaël Brouard and Vincent Rouffiange, "Unbroadened-spectrum chirped modulation: effects of the chirp-inducing mechanism on the spectral broadening in LiNbO3 modulators," IEEE Photon. Technol. Lett., vol. 17, 2005, pp. 564–566.

[10] Douglas M. Gill, Alan H. Gnauck, Xiang Liu XingWei, David S. Levy, S. Chandrasekhar and Christopher R. Doerr, "42.7-Gb/s cost-effective duobinary optical transmitter using a commercial 10-Gb/s Mach–Zehnder modulator with optical filtering," IEEE Photon. Technol. Lett., vol. 17, 2005, pp. 917-919 (2005).

[11] Shiva Kumar, Impact of Nonlinearities on Fiber Optic Communications, 1st ed., Canada, 2011.

[12] Christophe Peucheret and DTU Fotonik, Generation and Detection of Optical Modulation Formats, Department of Photonics Engineering Technical University of Denmark, 2012.

[13] Jhon M. Senior, Optical Fiber Communications Principles and Practice, Prentice Hall, UK, 2009.

[14] Milorad Cvijetic and Ivan B. Djordjevic, Advanced Optical Communications Systems and Networks, USA, 2013.

[15] Tasshi Dennis and Paul A. Williams, "Chirp characterization of external modulators with finite extinction ratio using linear optical sampling," IEEE Photon. Technol. Lett., vol. 22, 2010, pp. 646–648.

[16] Le Nguyen Binh and Itzhak Shraga, "An optical fiber dispersion measurement technique and system," technical report, Monash University, Australia, 2005.

[17] Hoon Kim and Alan H. Gnauck, "Chirp characteristics of dual-drive Mach–Zehnder modulator with a finite DC extinction ratio," IEEE Photon. Technol. Lett., vol. 14, 2002, pp.298-300.

[18] Tasshi Dennis and Paul A. Williams, "Chirp characterization of external modulators with finite extinction ratio using linear optical sampling," IEEE Photon. Technol. Lett., vol. 22, 2010, pp. 646–648.